Journal of Sciences, Islamic Republic of Iran 30(1): 13 - 21 (2019) http://jsciences.ut.ac.ir
University of Tehran, ISSN 1016-1104

Effect of Calcination Rate on Performance of Co-precipitated Cu-MgO Catalyst in Hydrogenation of Furfural

M. Ghashghaee[*1,2], S. Shirvani[1,2], S. Sadjadi[2,3], V. Farzaneh[1,2]

[1] *Faculty of Petrochemicals, Iran Polymer and Petrochemical Institute, P.O. Box 14975-112, Tehran, Islamic Republic of Iran*
[2] *Biomass Conversion Science and Technology (BCST) Division, Iran Polymer and Petrochemical Institute, P.O. Box 14975-115, Tehran, Islamic Republic of Iran*
[3] *Gas Conversion Department, Faculty of Petrochemicals, Iran Polymer and Petrochemical Institute, P.O. Box 14975-112, Tehran, Islamic Republic of Iran*

Received: 3 January 2017 / Revised: 22 May 2017 / Accepted: 12 August 2017

Abstract

Co-precipitated Cu-MgO catalysts were prepared and evaluated for the gas-phase hydrogenation of furfural. The effect of heating rate at the calcination step was studied by comparing the performance of three catalysts prepared via the same procedure but calcined at different heating rates. The results established that altering the heating rate could influence the structural properties of the catalyst samples and hence their activity and selectivity. An extremely poor catalytic activity and selectivity (lower than 0.1% conversion of furfural and 40% selectivity towards furfuryl alcohol after 240 min time-on-stream) belonged to the catalyst that was prepared with the lowest calcination rate (1 Kmin–1), while the other two catalysts prepared with the calcination rate of 5 and 10 Kmin–1 indicated more than 88% conversion of furfural and 85% furfuryl alcohol selectivity during this run length.

Keywords: Hydrogenation; Furfural; Furfuryl alcohol; Copper; Calcination.

Introduction

With the increase of global energy demand and depletion of fossil fuel reserves [1-3] as well as environmental problems such as increase of green house gases and consequently global warming [4], it is imperative to use renewable resources. In this context, biomass is assumed as a promising alternative to fossil fuel [5-10]. In the past few decades many efforts have been devoted to the conversion of biomass-derived compounds to fine chemicals and fuels [11,7,12-13,9].

Furfural (FF), a lignocellulose derivative, is a promising platform chemical which can be used as an adhesive, fungicide, nematocide and extracting agent [14-17,8,18]. Additionally, it can be transformed into value-added chemicals and fuel components such as furfuryl amine, furan, linear alkanes, furoic acid, 2-methyl tetrahydrofuran, 2-methylfuran, tetrahydro-furfuryl alcohol, 1,5-pentanediol, cyclopentanone, maleic acid, and mainly furfuryl alcohol [19-20,4,8,21,15]. Furfuryl alcohol (FFA) can be used for the manufacture of thermostatic resins, furanic fiber-

* Corresponding author: Tel: +982148662481; Fax: +982144787032; Email: m.ghashghaee@ippi.ac.ir

reinforced plastics, liquid and foundry resins, adhesives, ascorbic acid, farm chemicals, lysine, dispersing agents, and lubricants [22-24,9].

Hydroconversionof FF to FFA can be performed in liquid [24-26,16] or gas [23,27,10,28-29] phases. However, the gas-phase hydrogenation is preferred as it can be carried out at ambient pressure [21,30]. In addition, it does not have the risk of organic solvents applied in the liquid phase hydrogenation process. Instead, the vast range of byproducts which are obtained even in trace amounts and also the higher energy consumption due to the FF vaporization are regarded as its drawbacks [31].

Industrially, hydrogenation of FF is performed in the gas phase at moderate temperatures (403–473 K) and pressures up to 30 atm using commercial copper chromite catalyst [32]. Although copper chromiteexhibits high selectivity to FFA, its toxic nature as well as its moderate activity, provoked huge attempts for developing alternative Cr-free catalysts containing Cu, Ni, Ru, Ir, Pt, Co, and Pd supported on different materials such as SiO_2 and Al_2O_3 [33,4,34-36,17].

In this regard, the Cu-MgO catalyst proposed by Nagaraja et al. in 2007 has attracted growing interest due to its relatively low cost, substantial activity and high selectivity to FFA [21,23,37-40,33,41]. Several reports with the approach of investigating the effects of various parameters on the performance of co-precipitated or impregnated Cu-MgO catalysts have recently been published [42,28,43-44].

In this paper, the effects of heating rate at the calcination step on the activity of the synthesized co-precipitated Cu-MgO catalyst were evaluated for the first time. Reaction data were obtained by altering the heating rate from 1 to 10 $Kmin^{-1}$ at three levels followed by applying the synthesized catalysts to the FF hydrogenation process and calculating the performance parameters such as FF conversion, FFA yield and selectivity. Another goal of this study was to figure out how the heating rate at the calcination step affects the structural properties and performance of the synthesized catalyst.

Materials and Methods

Materials

All chemicals employed for synthesis of the samples were used directly without further purification. $Cu(NO_3)_2.3H_2O$ (99.5%), $Mg(NO_3)_2.6H_2O$ (ACS reagent, 99%) and K_2CO_3 (ACS reagent, 99.5%), were purchased from Merck. The material used for the catalytic reactions included FF (98.6%, Behran Oil Co.) and high purity H_2 (99.99%) and N_2 (99.99%).

Catalyst preparation

The copper catalysts were prepared using the starting precursors with the mass ratio of 16:84 for Cu:MgO via co-precipitation. In a typical preparation, a mixture of 1 M solution of $Cu(NO_3)_2.3H_2O$ and $Mg(NO_3)_2.6H_2O$ was allowed to precipitate at a pH of 9.0 by the addition of 1 M solution of K_2CO_3 at ambient temperature. The resulting solution was stirred for 3 h. Subsequently, the precipitate was filtered and washed with distilled water and dried at 393 K for 15 h. The dried powder was calcined in air at 723 K for 5 h with the heating rates of 1, 5, and 10 $Kmin^{-1}$. The resulting catalyst samples were named as CM1, CM5, and CM10, respectively.

Catalyst and products characterization

Characterization of prepared catalysts was performed using SEM/EDX, BET, and XRD analyses. Tescan instrument, using Au-coated samples with an acceleration voltage of 20 kV was employed for obtaining SEM/EDX images. Room temperature powder X-ray diffraction patterns were collected using a Siemens D5000. Cobalt Co Kα radiation was used from a sealed tube. Data were collected in the 2θ range of 10–88° with a step size of 0.02° and an exposure time of 2s per step. To measure the BET surface areas via nitrogen physisorption, a Quantachrome Chem-BET 3000 sorption analyzer was used. Degassing of the samples was carried out at 393 K for 3 h. The reaction products were analyzed on a gas chromatograph (GC) equipped with a capillary column and a flame ionization detector (FID).

Catalytic activity

Hydrogenation of FF was carried out in a tubular reactor of 10-mm internal diameter. The catalyst pellets were placed in the reactor. The catalyst was initially reduced in a flow of hydrogen (33 vol.%) dilued with nitrogen with a total flow rate of 6420 $mLg^{-1}h^{-1}$ at 523 K for 3 h. Then, the catalyst bed was cooled down to the reaction temperature in H_2 and subsequently the feedstock (FF) was injected into the reactor using a micro-feeder pump. The reaction conditions were 453 K, hydrogen-to-hydrocarbon (H_2/HC) volumetric ratio of 10.6, WHSV of 1.7 h^{-1}, and atmospheric pressure. The carbon balance was always better than 95% unless otherwise mentioned. Finally, the performance of the catalyst was evaluated using the following definitions:

$$\text{Conversion (\%)} = (n_{FF,in} - n_{FF,out})/n_{FF,in} \times 100 \quad (1)$$

$$\text{Selectivity (mol\%)} = n_{Product,out} /(n_{FF,in} - n_{FF,out}) \times 100 \quad (2)$$

$$\text{Yield (mol\%)} = n_{Product,out} /n_{FF,in} \times 100\% \quad (3)$$

where *n* denotes the number of moles of the given species at the reactor inlet (in) or outlet (out).

Results and Discussion

Figure 1 illustrates the reaction results for the hydrogenation of FF over the synthesized catalysts.

Interestingly, the sample prepared with the lowest heating rate (CM1) was the least active catalyst. Although the selectivity to FFA and the FF conversion were 100% and ~16% at 60 min, both of them decreased dramatically with time-on-stream. The other two catalysts (CM5 and CM10) were almost equally efficient in the selective conversion of FF to FFA. More precisely, CM10 was a little more active (giving conversion levels over 95% at 60 min) than CM5 while CM5 was slightly more selective (over 97% FFA selectivity at 240 min) than CM10, thus eventually giving FFA yields of up to 87.5%. Indeed, the activity and selectivity of these two catalysts were almost stable during 240 min time-on-stream. Overall, one might conclude that a heating rate of 5 $Kmin^{-1}$ or higher is favored in terms of conversion, selectivity, and durability.

Figure 2 displays the trends of the statistically significant byproducts obtained from the reactions on the catalysts. The major components obtained in the product stream at 240 min on CM1 were 2-methylfurfural (~60%) and FFA (~40%). Except CM1, the synthesized catalysts demonstrated an increasing magnitude of selectivity to FFA with time. It is evident that this climbing trend has been concurrent with a decrease in the selectivities of the other products. As indicated by these charts, the main reaction pathways that reduced the FFA selectivity on CM5 and CM10 were those leading to tetrahydrofurfuryl alcohol (THFA), 1-pentanol (1POL), and furfuryl ether (FFE). An increase in the heating rate from 5 to 10 $Kmin^{-1}$ made the Cu-MgO catalyst more selective to THFA while producing no FFE. This indicates that the change in the heating rate of calcination is capable of changing the product slate. In any event, one could state that the reactions that produced these compounds have been set back as the active sites engaged in these reactions were covered, e.g., by coke species with the operation time, thus leading to improved selectivities of FFA. One might anticipate that the loss in some active sites would reduce the whole activity. However, this partial coverage of active sites was not unfavorable to the desired alcohol yield (Fig. 1), which is the most important measure for the catalytic activity.

Figure 3 demonstrates the other important byproducts which included 2-methyltetrahydrofuran (MTHF), 2,3-dihydro-5-methylfuran (DHMF), 1,2-pentanediol (12PDO), 2-acetylfuran (AF), 5-methylfurfuryl alcohol (MFFA), γ-valerolactone (GVL), and δ-valerolactone (DVL) as shown in Fig. 3. As can be seen in this figure, CM10 led to the highest THFA while CM5 presented the highest selectivity to FFE and CM1 showed the largest AF production in terms of averaged product selectivities.

To elucidate the origin of the differences in the catalytic behavior and disclose the effect of calcination heating rate on the structural properties of the catalysts, all catalysts were analyzed using XRD, SEM/EDX, and BET techniques. The comparison of the surface areas of the samples (Table 1) indicated that the sample calcined at the lowest heating rate, CM1, presented the lowest

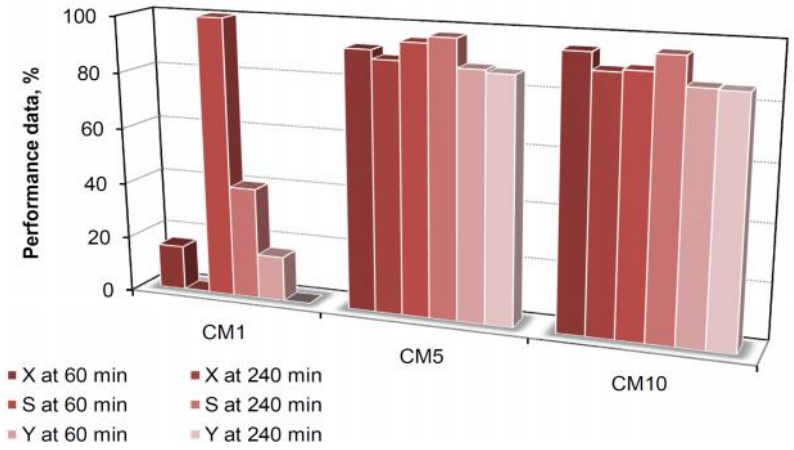

Figure 1. Effect of heating rate on the catalytic hydrogenation of FF to FFA over the Cu-MgO catalysts prepared with different calcination rates. The reaction conditions were 453 K, 1 atm, WHSV of 1.7 h^{-1}, and H_2/HC of 10.6 (labels X, S, and Y show conversion, selectivity, and yield, respectively).

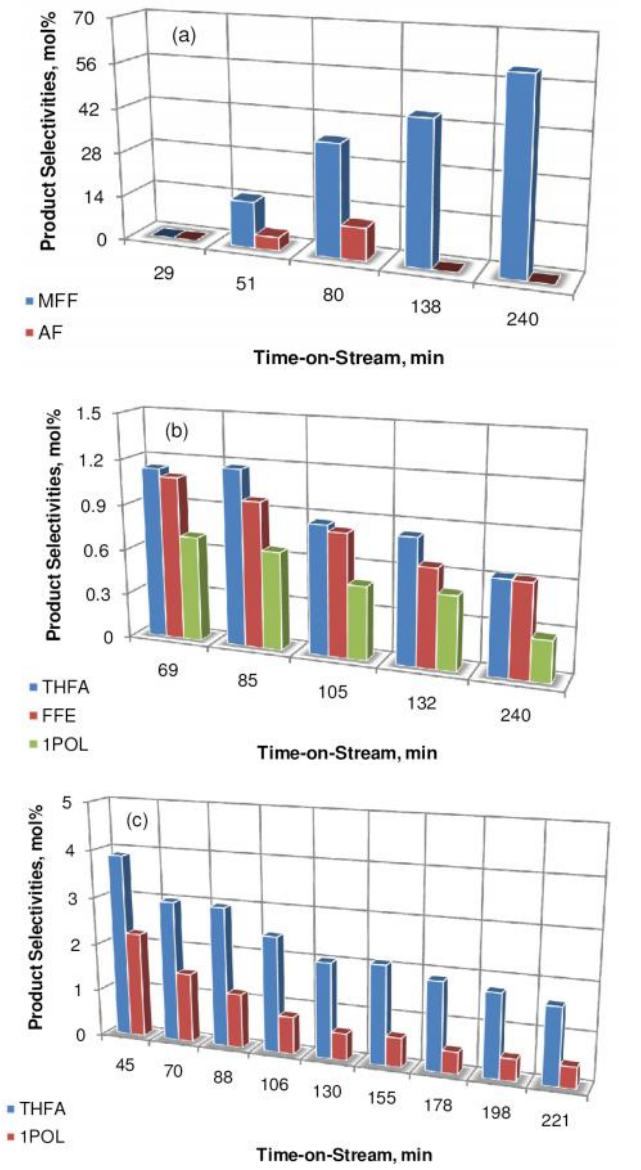

Figure 2. Major byproducts obtained from (a) CM1, (b) CM5, and (c) CM10. The experimental conditions were 453 K, 1 atm, WHSV of 1.7 h^{-1}, and H_2/HC of 10.6.

BET surface area (47.56 m^2g^{-1}) while the catalyst prepared with the heating rate of 5 $Kmin^{-1}$ had the highest BET surface area (102.26 m^2g^{-1}). These results proved that the calcination heating rate could considerably affect the BET surface area as also proven in the previous research [45-47]. However, there was no linear relationship between the heating rate at calcinations step and the BET surface area. Upon increasing the calcination rate from 1 $Kmin^{-1}$ to 5 $Kmin^{-1}$, an approximately twofold increase was observed in the BET surface area. Nonetheless, this trend was not steady and the BET surface area decreased significantly at the heating rate of 10 $Kmin^{-1}$ [45].

The SEM/EDX mapping analyses of the samples are shown in Fig. 4. As is evident, the SEM images of the catalysts demonstrated demonstrated that changing the heating rate at the calcination step could clearly affect the catalysts morphologies. Calcination of the catalyst at the heating rate of 1 $Kmin^{-1}$ brought about a rod-like morphology as well as aggregates. Upon increasing the heating rate to 5 $Kmin^{-1}$, the rod-like morphology was disappeared and only aggregates were observed.

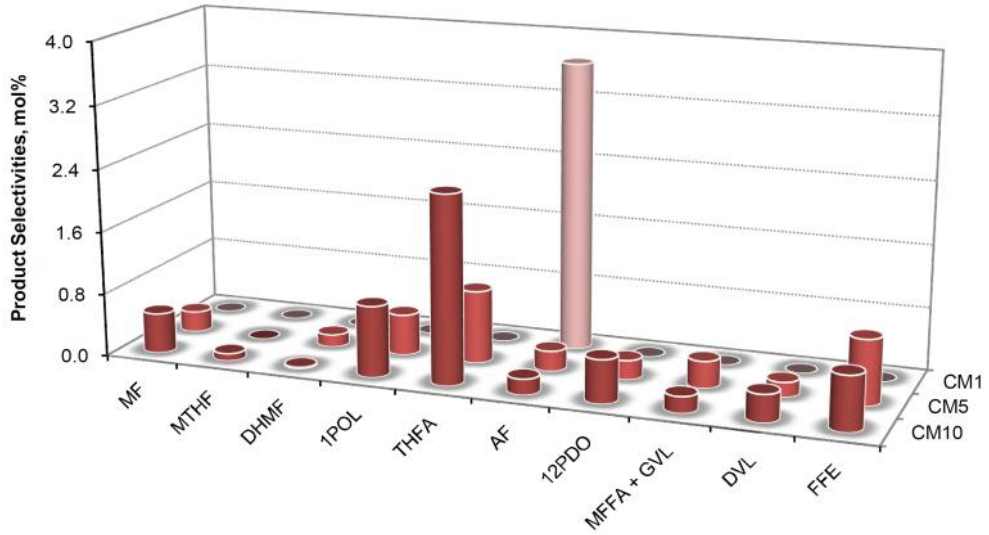

Figure 3. Overall selectivities to different byproducts with CM1, CM5, and CM10 over 240 min of operation

Table 1. Textural properties (crystal size and surface area) of the Cu-MgO catalysts

Sample	CuO crystallite size (nm)	Surface area (m^2g^{-1})
CM1	17.8	47.56
CM5	6.2	102.26
CM10	7.2	69.35

Atelevated calcination rates, viz. 10 $Kmin^{-1}$, however, the rod-like morphology appeared again. Taking the BET surface area data into account, one can conclude that the presence and abundance of the rod-like morphology has led to a lower BET surface area. Conversely, the formation of porous aggregates increased the area of the obtained catalyst.

The presence of the Cu, Mg and O atoms in the EDX analyses of all three catalysts established the possible formation of the desired Cu-MgO catalysts as confirmed by their atomic distribution on the surface. The results of elemental mapping analysis indicated that in CM1 catalyst which exhibited the lowest catalytic activity, the Mg had the poorest dispersion while in CM5 and CM10 which showed almost similar activities, the dispersion of the Cu and Mg elements were almost similar. More precisely, the dispersion of active species is slightly better in CM5 sample. Considering the SEM images of the three catalysts, it can be postulated that the formation of rod-like morphology which mightresult in the decrease of BET surface area in comparison to the sample with porous aggregates, prevented the active species from well dispersion and consequently decreased the catalytic activity.

Figure 5 shows the XRD patterns of the three synthesized catalysts. The position and relative intensities of all peaks confirm well with the standard patterns of MgO (JCPDS card No. 45-0946) and CuO (JCPDS card No. 05-0661 and 78-0428). It can be seen that changing the heating rate can also influence the XRD patterns of the samples.

The calculated sizes for the CuO crystals in the samples are listed in Table 1. The values indicated that CM5 and CM1 possessed the smallest (6.2 nm) and the largest (17.8 nm) CuO crystallite sizes, respectively. In the case of CM10, this value for was 7.2 nm which was close to that of CM5. The high dispersion of elements on the surface of CM5 which was observed in its elemental mapping could be attributed to the small crystallite size of CuO in this catalyst. The low surface area which possibely emerged from the formation of rod-like morphology and consequently the poor dispersion on the surface can accordingly rationalize the large CuO crystallite size observed for the CM1 sample. Based on the structural analyses, the higher catalytic performance of CM5 could then be attributed to its higher surface area, lower crystallite size, and high dispersion.

In order to elucidate the preferences of the Cu-MgO catalyst compared to the reference commercial copper chromite catalyst, the results of hydrogenation of FF to FFA are mentioned in Table 2. As evident, the synthesized catalyst operated better in terms of both yield of FFA and catalytic stability.

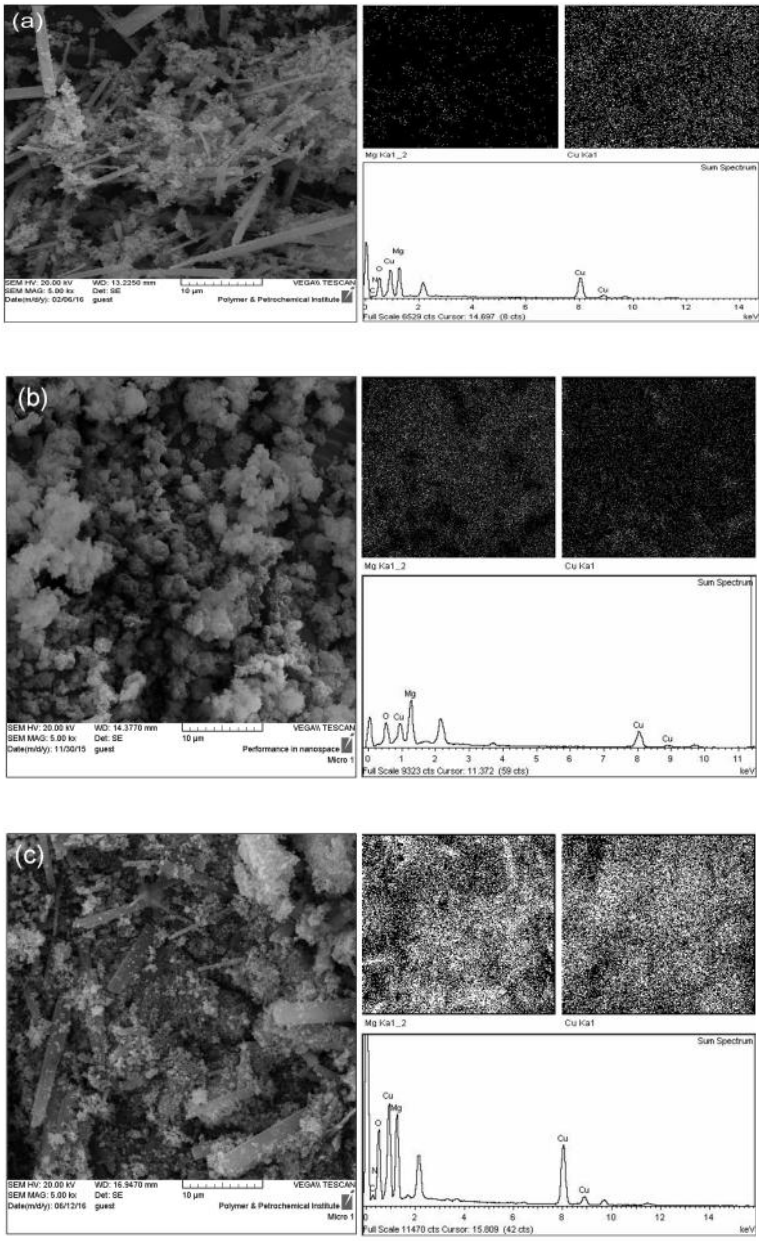

Figure 4. SEM/EDX mapping of the Cu-MgO catalysts: (a) CM1, (b) CM5, and (c) CM10

In summery the effect of heating rate at the calcination step on the activity and selectivity of the co-precipitated Cu-MgO catalyst in the catalytic hydrogenation of furfural was studied in detail.

Three samples (CM1, CM5, and CM10) were prepared in the same manner but calcined at different heating rates of 1, 5, and 10 $Kmin^{-1}$, respectively. The characterization of the prepared catalysts established that altering the heating rate could clearly affect the structural features of the catalysts including morphology, BET surface area, and crystallite size. The experiments at atmospheric conditions, 453 K and WHSV of 1.7 h^{-1} led to the conclusion that CM1 has been the least active catalyst while CM5 and CM10 were almost equally efficient (both of them showed more than 88% FF conversion and 85% FFA selectivity during the operation). However, CM5 that showed the highest selectivity to FFA was found as the catalyst of choice. Interestingly, altering the heating rate could also influence the distribution of the byproducts. The higher

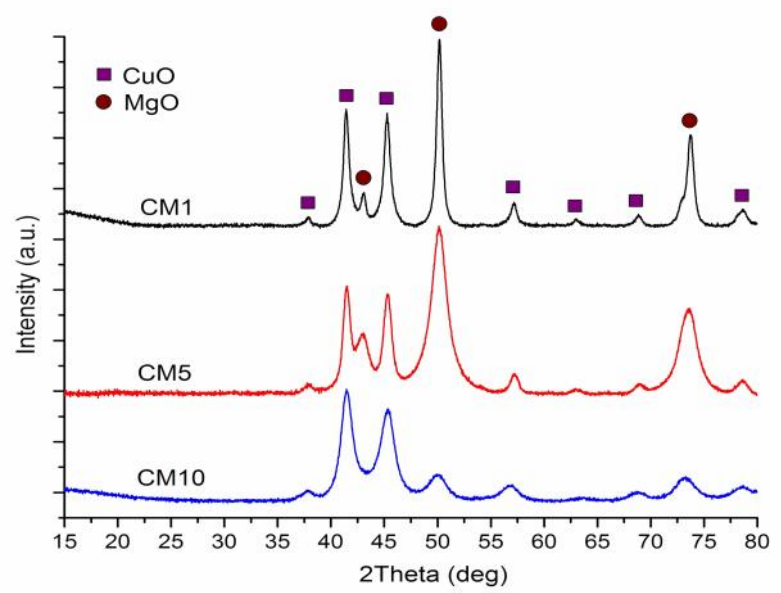

Figure 5. XRD patterns obtained for the three Cu-MgO catalysts

Table 2. Comparison of copper-magnesium oxide catalyst with the conventional copper chromite catalyst applied commercially to the hydrogenation of furfural

Catalyst	Temp. (K)	H_2/HC	Conversion (%)	Selectivity (%)	Yield (%)	Stability	Ref.
Cu-1800P	473	25	22	91.2	20	Poor	[48]
Copper-Chromite	473	25	98.2	18	17.7	Poor	[18]
Cu-1800P	453	—	46	65	30	—	[49]
CM5	453	10.6	88.8	97.4	86.5	Very Good	This study

catalytic performance of CM5 was attributed to its higher surface area, lower crystallite size, and high dispersion of active speices on the surface of the catalyst.

Acknowledgment

The authors appreciate the financial support from Iran Polymer and Petrochemical Institute.

References

1. Zhang X., Tu M. and Paice M.G. Routes to Potential Bioproducts from Lignocellulosic Biomass Lignin and Hemicelluloses. *Bioenerg Res.*, **4**(4):246–257 (2011).
2. Dutta S., De S., Saha B. and Alam M.I. Advances in conversion of hemicellulosic biomass to furfural and upgrading to biofuels. *Catal. Sci. Technol.*, **2**(10):2025–2036 (2012).
3. Yu W., Tang Y., Mo L., Chen P., Lou H. and Zheng X. One-step hydrogenation–esterification of furfural and acetic acid over bifunctional Pd catalysts for bio-oil upgrading. *Bioresource Technol.*, **102**(17):8241–8246 (2011).
4. Halilu A., Ali T.H., Atta A.Y., Sudarsanam P., Bhargava S.K. and Abd Hamid S.B. Highly Selective Hydrogenation of Biomass-Derived Furfural into Furfuryl Alcohol Using a Novel Magnetic Nanoparticles Catalyst. *Energ. Fuel.*, **30**(3):2216–2226 (2016).
5. Nakagawa Y., Tamura M. and Tomishige K. Catalytic Reduction of Biomass-Derived Furanic Compounds with Hydrogen. *ACS Catal.*, **3**(12):2655–2668 (2013).
6. Triebl C., Nikolakis V. and Ierapetritou M. Simulation and economic analysis of 5-hydroxymethylfurfural conversion to 2,5-furandicarboxylic acid. *Comput. Chem. Eng.*, **52**(0):26–34 (2013).
7. Wettstein S.G., Alonso D.M., Gürbüz E.I. and Dumesic J.A. A roadmap for conversion of lignocellulosic biomass to chemicals and fuels. *Curr. Opin. Chem. Eng.*, **1**(3):218–224 (2012).
8. Jiménez-Gómez C.P., Cecilia J.A., Durán-Martín D., Moreno-Tost R., Santamaría-González J., Mérida-Robles J., Mariscal R. and Maireles-Torres P. Gas-phase hydrogenation of furfural to furfuryl alcohol over Cu/ZnO catalysts. *J. Catal.*, **336**:107–115 (2016).
9. Taylor M.J., Durndell L.J., Isaacs M.A., Parlett C.M.A., Wilson K., Lee A.F. and Kyriakou G. Highly selective

hydrogenation of furfural over supported Pt nanoparticles under mild conditions. *Appl. Catal. B-Environ.*, **180**:580–585 (2016).
10. Yan K. and Chen A. Efficient hydrogenation of biomass-derived furfural and levulinic acid on the facilely synthesized noble-metal-free Cu–Cr catalyst. *Energy.* **58**:357–363 (2013).
11. Climent M.J., Corma A. and Iborra S. Conversion of biomass platform molecules into fuel additives and liquid hydrocarbon fuels. *Green Chem.*, **16**(2):516–547 (2014).
12. Ulbrich K. The Conversion of Furan Derivatives from Renewable Resources into valuable Building Blocks and their Application in Synthetic Chemistry. PhD, University of Regensburg, (2014).
13. Zhu S., Xue Y., Guo J., Cen Y., Wang J. and Fan W. Integrated Conversion of Hemicellulose and Furfural into γ-Valerolactone over Au/ZrO_2 Catalyst Combined with ZSM-5. *ACS Catal.*, **6**(3):2035–2042 (2016).
14. Lange J. P., van der Heide E., van Buijtenen J. and Price R. Furfural—A Promising Platform for Lignocellulosic Biofuels. *ChemSusChem*, **5**(1):150–166 (2012).
15. Manikandan M., Venugopal A.K., Nagpure A.S., Chilukuri S. and Raja T. Promotional effect of Fe on the performance of supported Cu catalyst for ambient pressure hydrogenation of furfural. *RSC Adv.*, **6**(5):3888–3898 (2016).
16. Li J., Liu J. L., Zhou H. J. and Fu Y. Catalytic Transfer Hydrogenation of Furfural to Furfuryl Alcohol over Nitrogen-Doped Carbon-Supported Iron Catalysts. *ChemSusChem*, **9**(11):1339–1347 (2016).
17. Aldosari O.F., Iqbal S., Miedziak P.J., Brett G.L., Jones D.R., Liu X., Edwards J.K., Morgan D.J., Knight D.K. and Hutchings G.J. Pd–Ru/TiO_2 Catalyst–an Active and Selective Catalyst for Furfural Hydrogenation. *Catal. Sci. Technol.*, **6**(1):234–242 (2016).
18. Zhang H., Canlas C., Kropf A.J., Elam J.W., Dumesic J.A. and Marshall C.L. Enhancing the Stability of Copper Chromite Catalysts for the Selective Hydrogenation of Furfural with ALD Overcoating (II)–Comparison between TiO_2 and Al_2O_3 Overcoatings. *J. Catal.*, **326**:172–181 (2015).
19. Yan K., Wu X., An X. and Xie X. Novel Preparation of Nano-Composite CuO-Cr2O3 Using CTAB-Template Method and Efficient for Hydrogenation of Biomass-Derived Furfural. *Funct Mater Lett*, **6**(01):1350007-1350001–1350007-1350005 (2013).
20. Sulmonetti T.P., Pang S.H., Claure M.T., Lee S., Cullen D.A., Agrawal P.K. and Jones C.W. Vapor phase hydrogenation of furfural over nickel mixed metal oxide catalysts derived from layered double hydroxides. *Appl. Catal. A-Gen.*, **517**:187–195 (2016).
21. Vargas-Hernández D., Rubio-Caballero J.M., Santamaría-González J., Moreno-Tost R., Mérida-Robles J.M., Pérez-Cruz M.A., Jiménez-López A., Hernández-Huesca R. and Maireles-Torres P. Furfuryl alcohol from furfural hydrogenation over copper supported on SBA-15 silica catalysts. *J Mol. Catal. A-Chem.*, **383–384**:106–113 (2014).
22. Xu Y., Qiu S., Long J., Wang C., Chang J., Tan J., Liu Q., Ma L., Wang T. and Zhang Q. In Situ Hydrogenation of Furfural with Additives over a Raney Ni Catalyst. *RSC Adv.*, **5**(111):91190–91195 (2015).
23. Nagaraja B.M., Padmasri A.H., David Raju B. and Rama Rao K.S. Vapor phase selective hydrogenation of furfural to furfuryl alcohol over Cu–MgO coprecipitated catalysts. *J. Mol. Catal. A.*, **265**(1–2):90–97 (2007).
24. Yuan Q., Zhang D., van Haandel L., Ye F., Xue T., Hensen E.J.M. and Guan Y. Selective liquid phase hydrogenation of furfural to furfuryl alcohol by Ru/Zr-MOFs. *J. Mol. Catal. A-Chem.*, **406**:58–64 (2015).
25. Sharma R.V., Das U., Sammynaiken R. and Dalai A.K. Liquid phase chemo-selective catalytic hydrogenation of furfural to furfuryl alcohol. *Appl Catal A-Gen*, **454**:127–136 (2013).
26. Villaverde M.M., Garetto T.F. and Marchi A.J. Liquid-phase transfer hydrogenation of furfural to furfuryl alcohol on Cu–Mg–Al catalysts. *Catal. Commun.*, **58**:6–10 (2015).
27. Li M., Hao Y., Cárdenas-Lizana F. and Keane M.A. Selective production of furfuryl alcohol via gas phase hydrogenation of furfural over Au/Al_2O_3. *Catal. Commun.*, **69**:119–122 (2015).
28. Sadjadi S., Farzaneh V., Shirvani S. and Ghashghaee M. Preparation of Cu-MgO catalysts with different copper precursors and precipitating agents for the vapor-phase hydrogenation of furfural. *Korean J. Chem. Eng.*, **34**(3):692–700 (2017).
29. Ghashghaee M., Shirvani S. and Farzaneh V. Effect of Promoter on Selective Hydrogenation of Furfural over Cu-Cr/TiO_2 Catalyst. *Russ. J. Appl. Chem.*, **90**(2):304–309 (2017).
30. Shirvani S. and Ghashghaee M. Mechanism Discrimination for Bimolecular Reactions: Revisited with a Practical Hydrogenation Case Study. *Phys. Chem. Res.*, **5**(4):727–736 (2017).
31. Villaverde M.M., Bertero N.M., Garetto T.F. and Marchi A.J. Selective liquid-phase hydrogenation of furfural to furfuryl alcohol over Cu-based catalysts. *Catal. Today.*, **213**:87–92 (2013).
32. Kijeński J., Winiarek P., Paryjczak T., Lewicki A. and Mikołajska A. Platinum deposited on monolayer supports in selective hydrogenation of furfural to furfuryl alcohol. *Appl. Catal. A-Gen.*, **233**(1–2):171–182 (2002).
33. Nagaraja B.M., Padmasri A.H., Raju B.D. and Rama Rao K.S. Production of hydrogen through the coupling of dehydrogenation and hydrogenation for the synthesis of

cyclohexanone and furfuryl alcohol over different promoters supported on Cu–MgO catalysts. *Int. J. Hydrogen. Energ.*, **36**(5):3417–3425 (2011).

34. Nakagawa Y., Takada K., Tamura M. and Tomishige K. Total Hydrogenation of Furfural and 5-Hydroxymethylfurfural over Supported Pd–Ir Alloy Catalyst. *ACS Catal.*, **4**(8):2718–2726 (2014).
35. Lesiak M., Binczarski M., Karski S., Maniukiewicz W., Rogowski J., Szubiakiewicz E., Berlowska J., Dziugan P. and Witońska I. Hydrogenation of Furfural over Pd–Cu/Al_2O_3 Catalysts. The Role of Interaction between Palladium and Copper on Determining Catalytic Properties. *J. Mol. Catal. A-Chem.*, **395**:337–348 (2014).
36. 3An K., Musselwhite N., Kennedy G., Pushkarev V.V., Robert Baker L. and Somorjai G.A. Preparation of mesoporous oxides and their support effects on Pt nanoparticle catalysts in catalytic hydrogenation of furfural. *J. Colloid. Interf. Sci.*, **392**:122–128 (2013).
37. Nagaraja B.M., Kumar V.S., Shasikala V., Padmasri A.H., Sreedhar B., Raju B.D. and Rao K.S. A highly efficient Cu/MgO catalyst for vapour phase hydrogenation of furfural to furfuryl alcohol. *Catal. Commun.*, **4**(6):287–293 (2003).
38. Cui H., Wu X., Chen Y., Zhang J. and Boughton R.I. Influence of copper doping on chlorine adsorption and antibacterial behavior of MgO prepared by co-precipitation method. *Mater Res. Bull*, **61**:511–518 (2015).
39. Estrup A.J. Selective Hydrogenation of Furfural to Furfuyl Alcohol over Copper Magnesium Oxide. MSc, University of Maine, (2015).
40. Liu H., Hu Q., Fan G., Yang L. and Li F. Surface synergistic effect in well-dispersed Cu/MgO catalysts for highly efficient vapor-phase hydrogenation of carbonyl compounds. *Catal. Sci. Technol.*, **5**(8):3960–3969 (2015).
41. Ghashghaee M., Shirvani S. and Ghambarian M. Kinetic models for hydroconversion of furfural over the ecofriendly Cu-MgO catalyst: An experimental and theoretical study. *Appl. Catal. A-Gen.*, **545**:134–147 (2017).
42. 42. Ghashghaee M., Sadjadi S., Shirvani S. and Farzaneh V. A Novel Consecutive Approach for the Preparation of Cu–MgO Catalysts with High Activity for Hydrogenation of Furfural to Furfuryl Alcohol. *Catal. Lett.*, **147**(2):318–327 (2017).
43. Shirvani S., Ghashghaee M., Farzaneh V. and Sadjadi S. Influence of catalyst additives on vapor-phase hydrogenation of furfural to furfuryl alcohol on impregnated copper/magnesia. *Biomass Conv. Bioref.*:1–10 (2017).
44. Farzaneh V., Shirvani S., Sadjadi S. and Ghashghaee M. Promoting Effects of Calcium on the Performance of Cu-MgO Catalyst in Hydrogenation of Furfuraldehyde. *Iran J. Catal.*, **7**(1):53–79 (2017).
45. Feyzi M., Irandoust M. and Mirzaei A.A. Effects of promoters and calcination conditions on the catalytic performance of iron–manganese catalysts for Fischer–Tropsch synthesis. *Fuel Process Technol.*, **92**(5):1136–1143 (2011).
46. Rafiee H.R., Feyzi M., Jafari F. and Safari B. Preparation and Characterization of Promoted Fe-V/SiO_2 Nanocatalysts for Oxidation of Alcohols. *J. Chem.*, **2013**:10 (2013).
47. Schumann J., Behrens M., Schlögl R. and Schomäcker R. Cu, Zn-based catalysts for methanol synthesis. PhD Thesis, Technische Universität Berlin, Berlin (2015).
48. Liu D., Zemlyanov D., Wu T., Lobo-Lapidus R.J., Dumesic J.A., Miller J.T. and Marshall C.L. Deactivation mechanistic studies of copper chromite catalyst for selective hydrogenation of 2-furfuraldehyde. *J. Catal.*, **299**:336–345 (2013).
49. Nagaraja B.M., Aytam H.P., Podila S., Reddy K.H.P., Raju B.D. and Kamaraju S.R.R. A highly active Cu-MgO-Cr_2O_3 catalyst for simultaneous synthesis of furfuryl alcohol and cyclohexanone by a novel coupling route—Combination of furfural hydrogenation and cyclohexanol dehydrogenation. *J. Mol. Catal. A.*, **278**(1–2):29–37 (2007).